

NUMERICAL MODELING OF HETEROGENEOUS CARBONATES AND MULTI-SCALE DYNAMICS

Tuanfeng Zhang, Neil F. Hurley, and Weishu Zhao, Schlumberger-Doll Research

Copyright 2009, held jointly by the Society of Petrophysicists and Well Log Analysts (SPWLA) and the submitting authors.

This paper was prepared for presentation at the SPWLA 50th Annual Logging Symposium held in The Woodlands, Texas, United States, June 21-24, 2009.

ABSTRACT

A new state-of-the-art method, known as numerical pseudocores, bridges the gap between cores, borehole images, and numerical flow simulations to help solve the problem of carbonate reservoir heterogeneity.

Numerical pseudocores are 3D computer models of rocks and pores generated from borehole images and digital rock samples using multipoint statistics (MPS). Digital rock samples, created from computed-tomographic scans (CTscans), are used as training images. They are the quantitative templates used to guide MPS modeling of 3D textures in pseudocores. Borehole images surround numerical pseudocores with cylindrical envelopes that condition the models. Integer values are assigned to each petrophysical facies, for example, dense rock matrix is 0, vugs are 1, and electrically conductive patches are 2. Each numerical pseudocore absolutely honors the heterogeneities observed in digital rock samples and borehole images.

For each petrophysical facies, capillary pressure and relative permeability curves are provided by either conceptual models, special core analyses from plugs, or pore-network models from micron-scale CTscan images. Effective or bulk properties, such as porosity, permeability, residual oil saturations, relative permeabilities, and recovery factors can be deduced by running multiphase flow simulations through numerical pseudocores. Effective properties capture multi-scale heterogeneities in carbonates and provide essential constraints on interwell- or field-scale flow simulations.

INTRODUCTION

Carbonate reservoirs have heterogeneous pore-size distributions and permeabilities that range in scale over at least 6 orders of magnitude. Reservoir engineers have struggled for decades to quantify residual oil saturations, wettabilities, effective permeabilities, relative permeabilities, and recovery factors in such reservoirs.

Borehole images produce oriented electrical and acoustic maps of the rocks and fluids encountered by a well. Such logs provide the physical location of features such as bed boundaries, vugs, and porous vs. nonporous patches within the rocks. Patches outline 3D volumes that have complex shapes, known as petrophysical facies. Interpretation of these shapes is a key component in the analysis of centimeter- to meter-scale heterogeneities and their effect on fluid flow.

Digital rock samples are commonly constructed from various types of CTscans (conventional, microCT, and synchrotron-computed microtomography). CTscans are 2D cross sections generated by an X-ray source that rotates around the sample. Density is computed from X-ray attenuation coefficients. Scans of serial cross sections are used to construct 3D images of the samples. Because the density contrast is high between rocks and fluid-filled pores, CT images can be used to visualize the rock-pore system. Resolutions are on the millimeter to micron scale, depending on the device being used. Small sample size, unrepresentative of heterogeneous textures in carbonates, has been a major problem with previous digital rock models.

Multipoint statistics (MPS) creates simulations of spatial geological and reservoir property fields for subsurface reservoir modeling. These methods are conditional simulations that use known results measured in wellbores as fixed or “hard” data, which are absolutely honored during the simulations. MPS uses 1D, 2D, or 3D training images as quantitative templates to model subsurface property fields. MPS modeling captures geological structures from training images and anchors them to data locations. These structures can be *a priori* geological interpretations or conceptual models.

We use the pattern-recognition and modeling capabilities of MPS to create numerical pseudocores, which combine textures observed in borehole images with 3D pore distributions observed in digital rock samples. Numerical pseudocores are populated with porosity, permeability, capillary pressure, and relative permeability values for each discrete petrophysical facies. Multiphase flow simulations compute bulk, or system-scale properties such as residual oil saturations, capillary pressures, relative permeabilities, and

recovery factors to capture heterogeneous fabrics observed in carbonate reservoirs.

MULTIPOINT STATISTICS

Multipoint (or multiple-point) statistical methods (MPS) are a new family of spatial statistical interpolation algorithms proposed in the 1990s that are used to generate conditional simulations of discrete variable fields, such as geological facies, through training images (Guardiano and Srivastava, 1993). MPS is gaining popularity in reservoir modeling because of its ability to generate realistic models that can be constrained by different types of data. Unlike the conventional 2-point or variogram-based geostatistical approaches, MPS uses a training image to quantify complex depositional patterns believed to exist in studied reservoirs. These training patterns are then reproduced in the final MPS models with conditioning to local data collected from the reservoirs. Therefore, MPS allows modelers to use their prior geological interpretations as conceptual models (training images) in the reservoir modeling process and to evaluate the uncertainty associated with the prior interpretations by using different training images.

In addition to categorical variables, MPS can also be used to deal with continuously variable training images, such as spatial distribution of porosity. Two families of MPS algorithms are created to handle these different types of training images: Snesim for categorical variables, and Filtersim for continuous variables. Strebelle (2002) proposed an efficient Snesim algorithm that introduced the concept of a search tree to store all replicates of patterns found within a template over the training image. This makes Snesim code several orders of magnitude faster than the original algorithm proposed by Guardiano and Srivastava (1993). Filtersim, developed by Zhang (2006), applies a set of local filters to the training image, which can be either categorical or continuous, to group local patterns into pattern classes. Pattern simulation then proceeds on the basis of that classification.

Snesim and Filtersim algorithms honor absolute, or “hard” constraints from data acquired in wells or outcrops, and other interpreted trend maps of the reservoir under study. Training images are the main driver of any MPS approach. An issue raised implicitly by current MPS algorithms is how to generate training images. Training images are supposed to model or reproduce real geological features and should as much as possible be derived from existing geologically meaningful images. This requires research on statistical and image-processing methods that will allow use of images from any source: hand-drawn sketches, aerial

photographs, satellite images, seismic volumes, geological object-based models, physical-scale models, or geological process-based models.

Categorically variable training images are easier to generate than continuously variable training images. An object-based approach is commonly used to generate training images with categorical variables. A region-based approach, combined with the addition of desired constraints, can be used to generate continuously variable training images (Zhang *et al.*, 2006).

In this study, borehole images and digital core samples are directly taken as training images. These are discrete-variable training images, with the attribute being the rock (white) or pore (black) at each voxel of the image. The training image can have any shape of boundaries or contain any number of irregular holes.

FULLBORE IMAGES

Electrical and acoustic borehole-imaging tools are widely used to log subsurface boreholes to locate and map the boundaries between rock layers and to visualize and orient fractures and faults. Electrical borehole images can be acquired in water-based (conductive) mud, oil-based (nonconductive) mud, and in wireline or LWD (logging-while-drilling) modes.

Because most electrical borehole-imaging tools are pad-type devices with fixed arrays of electrodes, they commonly have gaps of missing information between the pads. Areal coverage of the borehole face is a function of the width of the electrode arrays, number of pads, and borehole diameter. In general, 40 to 80% of the borehole face is imaged in typical boreholes. Non-imaged parts of the borehole appear as blank strips between the pads. Gap width has generally decreased as new generations of tools and new tool combinations have been introduced.

Besides gaps between the pads, electrical and acoustic logs may have intervals with poor data quality because of borehole irregularities, washouts, thick mud cake, decentralized tools, or contamination by crushed rock materials.

Fullbore images (Hurley and Zhang, 2009) are used to fill the gaps or repair images with realistic statistical models. The method uses an MPS algorithm, such as Filtersim (Zhang, 2006) to generate fullbore images from borehole-image logs. Discrete, depth-defined intervals of borehole-image logs are used as training images. These training images are oriented, 2D scalar arrays of continuously variable numerical values, with

J
J
J

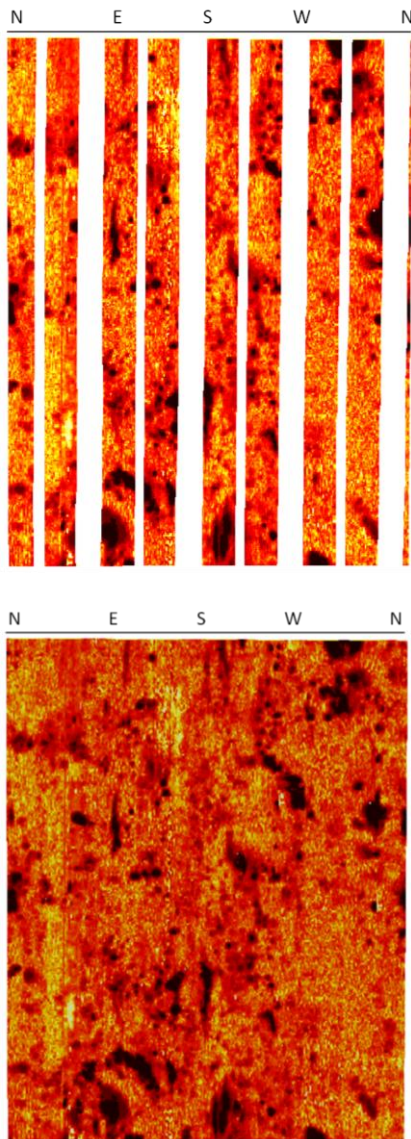


Fig. 1 Training image is a 3-ft (1-m) interval of a single-pass electrical borehole image (top) in a vuggy carbonate formation. Fullbore image (bottom) shows an MPS realization that uses the entire image on the top as a training image. The realization is conditioned so that it perfectly matches the original, measured data. Orientations are shown along the tops of the images. Abbreviations: N = north; E = east; S = south; and W = west. No vertical exaggeration. Bit size is 8.5 in (21.5 cm).

gaps between the pads or areas that need repair. The pads represent measured values and the gaps are non-imaged parts of the borehole.

Using Filtersim, we determine filter scores for each training image using a suitable pixel-based template. These scores quantify the patterns and their

probabilities, as observed in the measured data. We use filter scores to group and then simulate patterns in the gaps between the pads, where no measured data exist. Each realization is a fullbore image (Figure 1).

The approach for a single realization is to randomly occupy pixel locations and draw from the set of filter scores to choose a suitable pattern for the random site. Measured data are perfectly honored because these are conditional simulations. Patterns adjacent to the edges of pads match the patterns observed on the actual pads. The frequency distribution of modeled pixel colors, a continuous variable, perfectly matches the frequency distribution of measured colors. Multiple realizations of fullbore images honor the measured data in each realization, although subtle variations appear in the modeled areas. Wider gaps between pads result in more variations between realizations.

Finally, we scroll progressively through the entire logged interval, generating fullbore images from successive, adjacent, incomplete borehole images (training images).

PETROPHYSICAL FACIES

Vugs, which are large, irregular pores, visible to the naked eye, are common in carbonate rocks. Dehghani *et al.* (1999) suggested that zones of enhanced porosity and permeability exist in the vicinity of vugs. They used thin sections, SEM images, and minipermeability measurements to confirm this concept. Bourke (1993) showed that textures seen in borehole images closely resemble contoured minipermeability maps of cores. Schindler (2005) and Tanprasat (2005) used image analysis of fluorescent-inked core photos to show that swarms of small vugs preferentially exist in the vicinity of large vugs. Rathod (2003) used gridded minipermeability readings on core slabs to show that areas of enhanced permeability occur in the vicinity of vugs.

Small vugs are below the resolution of the borehole-imaging tool, so they appear as dark regions, rather than as discrete vugs in the image logs. If this is the general case for vuggy carbonates, electrical and acoustic borehole images should have high-conductivity or low-amplitude (dark) zones in the vicinity of vugs. In fact, this feature is commonly observed (for example, see Figure 2). Delhomme (1992) demonstrated the importance of mapping electrically resistive and nonresistive patches in borehole images. However, his approach was limited because of gaps between the pads. He was unable to draw closed contours around regions of high or low resistivity because of uncertainty about the shapes. Fullbore images allow us to draw closed

J
J
J

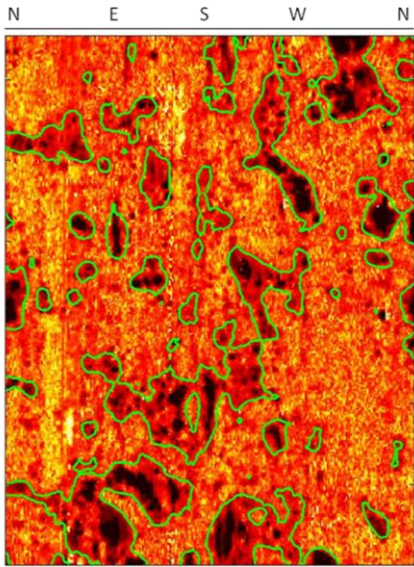


Fig. 2 Fullbore image of a 3-ft (1-m) interval in a vuggy carbonate formation (same as Figure 1) shows contours (green lines) that outline the less-resistive areas in the electrical image. Orientations are shown along the tops of the image. Abbreviations: N = north; E = east; S = south; and W = west. No vertical exaggeration. Bit size is 8.5 in (21.5 cm).

contours around resistive and/or nonresistive regions in borehole images. Such regions provide important measures of heterogeneity, especially in carbonate reservoirs, and are generally much larger than the core plugs or digital models we generate from CTscans of rocks. Because of this, borehole images are critical if we wish to identify and capture centimeter- to meter-scale heterogeneities in our flow models.

Regions with characteristic signatures on borehole-image logs, such as vugs, resistive patches, and conductive patches are herein termed petrophysical facies. Other authors, such as Ye *et al.* (1998) and Mathis *et al.* (2003) called similar textural regions electrofacies. Textures represented by different colors (as in Figure 2) can be used to define petrophysical facies, which have complex 3D shapes. Conductive patches, which correspond to zones of enhanced porosity and permeability, provide regions of flow continuity between vugs. As such, they help answer the question: “Are the vugs connected?”

DIGITAL MODELS OF ROCKS AND PORES

Published digital rock models are built using techniques that include: reconstructions from 2D thin sections or SEM (scanning-electron microscope) images, electrofacies interpreted from well logs, computer-generated

sphere packs, and various types of CTscans (conventional, microCT, and synchrotron-computed microtomography).

Oren and Bakke (2002), Dvorkin *et al.* (2003), and Okabe and Blunt (2005), among others, presented approaches to construct 3D pore networks from 2D thin sections. Tomutsa and Radmilovic (2007) used ion-beam thinning to create multiple 2D SEM serial sections, and built 3D models of submicron-scale pores.

Mathis *et al.* (2003) generated “synthetic cores” from a limited number of described cores, conventional openhole logs, and borehole-image logs, then constructed virtual electrofacies cores in non-cored wells. Creusen *et al.* (2007) described mini-models, or reservoir models that are less than 1.0 m³ in size that provide pseudo-properties for volume cells in reservoir-scale models. Abu-Shiekah *et al.* (2007) performed fine-scale numerical simulations of discrete rock types in a bioturbated carbonate core.

Behseresht *et al.* (2007), among others, described digital rock models that are computer-generated dense random periodic packings of spheres.

The most common way to generate pore networks is from various types of CTscans. Vinegar (1986), Wellington and Vinegar (1987), and Withjack *et al.* (2003) summarized the technology and discussed applications of X-ray computed tomography. Zhang *et al.* (2005), for example, generated conventional CTscan images of a vuggy limestone and performed flow simulations.

WORKFLOW FOR NUMERICAL PSEUDOCORE GENERATION

Our technique focuses on using the MPS algorithm Snesim to generate numerical pseudocores from digital rock samples and borehole-image logs. Our method includes a number of steps, discussed in the following sections:

- Select training images.
- Generate fullbore images.
- Warp fullbore images into scaled cylindrical shapes.
- Scale training images to fullbore images.
- Generate realizations of numerical pseudocores.
- Resample numerical pseudocores to radial grid.
- Perform flow simulations.

Select training images. Use digital rock samples with large volume, for example 4-inch diameter and 1 or 3 feet-length, as training images. These images can be

J
J
J

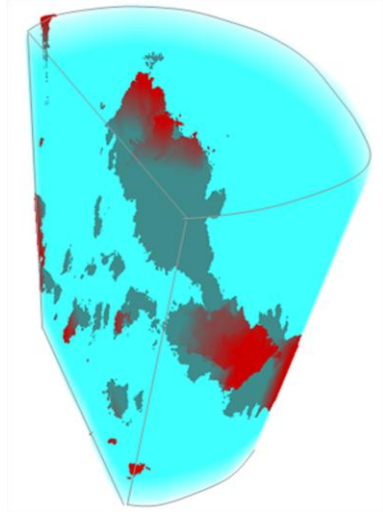


Fig. 3 Translucent, 3D view of CTscan of slabbed vuggy carbonate core sample. Vugs are red to gray in color, and dense rock matrix is blue. Height of the sample is 6 in (15 cm), and maximum diameter is 4 in (10 cm).

generated by CTscans with millimeter resolution and are considered to represent the heterogeneity distribution in the formation interval of the borehole under study. Training images are 3D arrays of discrete numerical values. In a 2-facies model, for example, the rock has a numerical value of 0, and the pores have a numerical value of 1. In a 3-facies model, the rock has a numerical value of 0, the pores have a numerical value of 1, and the conductive patches have a numerical value of 2. There is no limit on the number of facies. Outlines of individual facies bodies (volumes) can have any shape or size. However, one assumption should be justified before applying MPS: the training image used should contain representative patterns of the studied reservoir. In this study, the selected digital rock and its size are considered to be representative of the vug associations within a certain formation interval. To deal with distinct features that correspond to different formations or formation intervals, the proposed process can be repeated for different digital samples.

Figure 3 shows our chosen training image, a CTscan of a vuggy carbonate (Gowelly, 2003).

Generate fullbore images. Fullbore images (Hurley and Zhang, 2009) are already generated by certain logging tools, such as acoustic devices and LWD tools. In other cases, we must model fullbore images. This is especially true for resistivity logs, which commonly have gaps between the pads.

Our approach is to select a depth-defined interval of a borehole-image log. For example, this interval could be

1, 3, or 10 ft (0.3, 1, or 3 m) of measured depth. The user may want to choose a thick or thin interval, depending on the observed amount of layering, fracturing, and other heterogeneous patterns.

Figure 1 shows a fullbore image of vuggy porosity with contours (green lines, Figure 2) that outline dark-colored areas in the electrical image. These contours enclose conductive patches, similar to those cited by Delhomme (1992).

Numerical pseudocores can be conditioned to original, incomplete borehole images. However, the availability of fullbore images leads to a better-constrained model.

Warp fullbore images into scaled cylindrical shapes. For routine interpretations, it is difficult to examine borehole images in 3D. Therefore, the borehole is commonly split along true north, and the cylinder is unrolled until the view becomes 2D. In highly deviated and horizontal wells, the borehole image is commonly split along the top of the hole. Planar features that intersect the cylindrical borehole appear as sine waves in the 2D view.

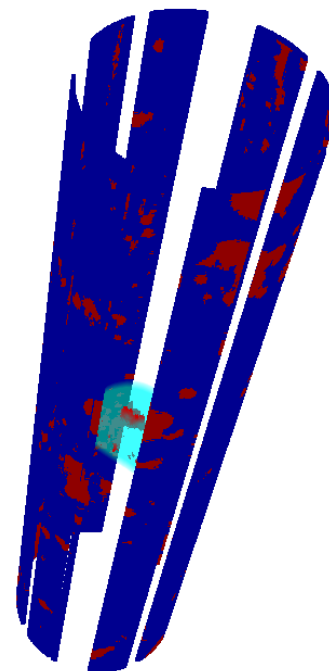


Fig. 4 Borehole images warped to cylindrical shape, matching the borehole diameter at this depth. Vugs are red, and dense rock matrix is blue. CTscan training image (same as Figure 3) is scaled and positioned at its correct depth in the center of the borehole images. Vugs are red and dense rock matrix is blue. Length of interval is 3 ft (1 m), and borehole diameter is 8.5 in (22 cm).

J
J
J

To generate 3D numerical pseudocores, we need to warp the 2D fullbore images back to their original 3D shape. To do this, we must know the borehole diameter. We can easily determine this from caliper logs run with the original borehole image. The image scale should be 1:1, that is, there should be no vertical exaggeration.

Figure 4 shows the borehole images warped to a 3D cylindrical shape. This figure does not show fullbore images to better convey the relative scales of the training image (CTscan, in the center of the cylinder) and the log image.

Scale training images to fullbore images. Typically, the voxel resolution of the digital rock or core training image is finer than the fullbore-image resolution. To ensure that the resulting pseudocore model has features at a scale consistent with the fullbore image, the training image is coarsely sampled according to the ratio of the resolutions of the digital core to the fullbore image, which is typically millimeter-scale resolution.

Figure 4 shows the rescaled training image, placed at its proper position with respect to the cylindrical borehole images.

Generate realizations of numerical pseudocores. We generate realizations of numerical pseudocores for two or more petrophysical facies using the Snesim algorithm of multipoint statistics. We condition the realizations to match the facies sizes and shapes observed in training images and fullbore images. Note that petrophysical facies can be defined from conductive patches seen in borehole images, even in sandstones or carbonates without vugs.

More than two petrophysical facies can be modeled in cases where conductive patches have been mapped in the borehole images and digital rocks. If the conductive patches have not been identified in the digital rocks (training images), they can be simulated by dilation of the porous facies by a fixed number of voxels. In this way, large-scale heterogeneity can be captured in the numerical pseudocore.

The size and height of the numerical pseudocore is limited only by the amount of computer memory that is available. In this case study, the pseudocore model consists of 30 million voxels with millimeter-scale resolution.

The simulation (one realization) of the numerical pseudocore (Figure 5) used fullbore images and a training image (Figure 4). Figure 6 shows slices through the numerical pseudocore to illustrate the true

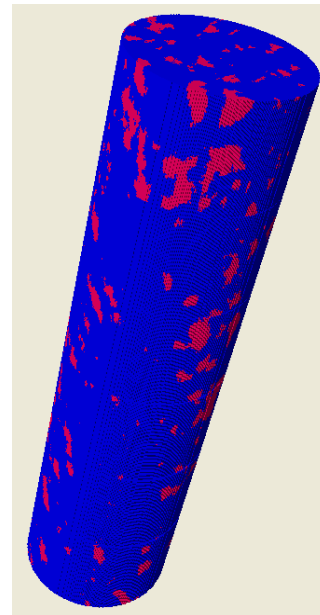


Fig. 5 Numerical pseudocore generated from training image in Figure 3 and fullbore images that correspond to Figure 1. Vugs are red, and dense rock matrix is blue. Length of interval is 3 ft (1 m), and borehole diameter is 8.5 in (22 cm).



Fig. 6 Numerical pseudocore generated from training image in Figure 3 and fullbore images that correspond to Figure 1. Vugs are clear, and dense rock matrix is gray. Length of interval is 1 ft (0.3 m), and borehole diameter is 8.5 in (22 cm). The arbitrary suspended slice (top) shows that this is truly a 3D model, with throughgoing pores in every slice.

J
J
J

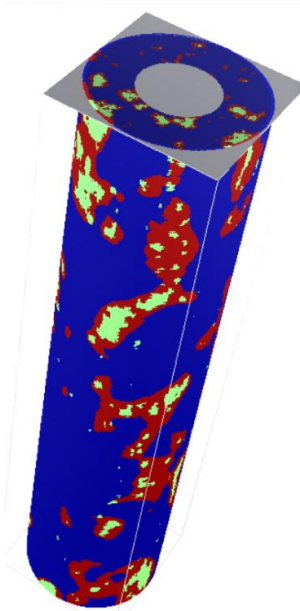


Fig. 7 Numerical pseudocore generated from training image in Figure 3 and fullbore images that correspond to Figure 1. Vugs are green, conductive patches are red, and dense rock matrix is blue. Conductive patches are similar to the contours shown in Figure 2. Length of interval is 3 ft (1 m), and borehole diameter is 8.5 in (22 cm).

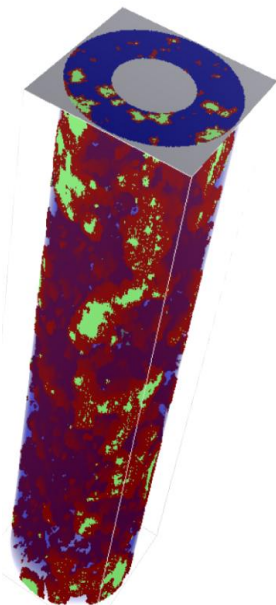


Fig. 8 Numerical pseudocore (same as Figure 7 but with dense rock matrix removed). Vugs are green, conductive patches are red, and the dense rock matrix is transparent. Length of interval is 3 ft (1 m), and borehole diameter is 8.5 in (22 cm).

3D nature of the model. Pores are present in any arbitrary slice taken through the model.

Figure 7 shows the numerical pseudocore with three facies: pores, conductive patches, and dense rock matrix. Conductive patches (red) are scaled to match contours around conductive patches shown in Figure 2. The conductive patches provide 3D connectivity between vugs, and they allow us to capture the heterogeneity that is inherent in most carbonate rocks.

Figure 8 shows the numerical pseudocore of Figure 7, with invisible transparent dense rock matrix. Note the 3D interconnected nature of the vugs and conductive patches.

Resample numerical pseudocores to radial grid. To conduct flow investigations of the numerical pseudocore, we regrid the model using the previous steps into a radial grid with cylindrical coordinates (Figure 9). Conversion to a radial grid is not required by our workflow. In fact, Cartesian flow simulations can be run. However, our goal is to simulate flow in the wellbore area, so we choose to resample the volume to a radial grid. Because running a numerical simulation is CPU-intensive, we conduct multiphase flow on only 1/3 of our pseudocore model (middle part) to investigate how geological heterogeneity associated with vug distribution influences fluid flow. In this example, resampling the numerical pseudocore model into a radial grid leads to a reduction of the size of the original static model from 10 million voxels ($n_x=259$, $n_y=231$, $n_z=510$) in the Cartesian grid to 250,000 voxels ($n_r=20$, $n_\theta=72$, $n_z=170$) in the radial grid.

At each Cartesian voxel, we assign a constant porosity and permeability according to its rock type (dense rock matrix, vug, or conductive patch). For each cell of the radial grid, because it consists of many Cartesian voxels, we generate average porosities and permeabilities. The average porosity is obtained by arithmetically averaging all porosity values of the Cartesian voxels within the cell; the average permeability is obtained by performing geometric averages of all permeability values.

Each Cartesian voxel in the numerical pseudocore belongs to a specific petrophysical facies (for example, dense rock matrix, vug, or conductive patch). We construct a look-up table of capillary pressure and relative permeability curves for each petrophysical facies (Figure 10). The source of the capillary pressure and relative permeability data can vary. Such curves can be provided by SCAL (Special Core AnaLysis) and MICP (Mercury-Injection Capillary Pressure) tests in the studied reservoir rocks. Alternatively, we can obtain

J
J
J

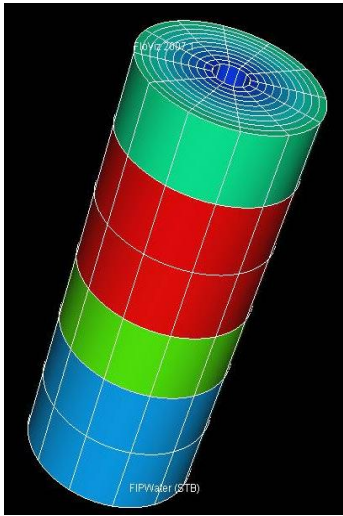


Fig. 9 Numerical pseudocores can be resampled or regrided to radial radial grids. Radial grids can be layered, based upon layers observed in borehole images or other well logs.

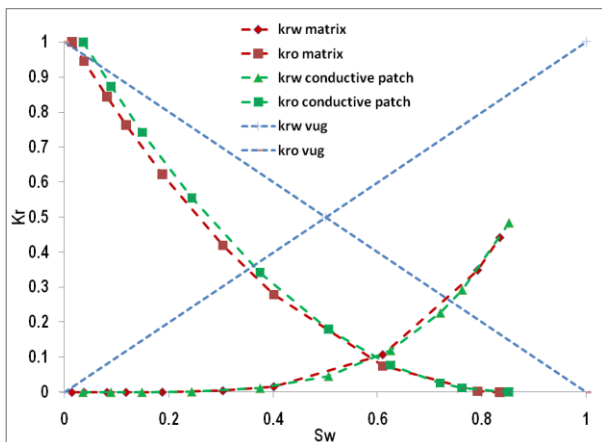


Fig. 10 Input relative permeability curves for different petrophysical facies.

values from similar reservoir rocks, for example, from a rock catalog. Capillary pressure and relative permeability curves can be generated from pore-network models, for example, Oren and Bakke (2002). Finally, we can construct conceptual curves, built to show water-wet, oil-wet, or mixed-wet conditions.

When we resample Cartesian voxels to the radial grid, we determine the dominant petrophysical facies in each radial grid cell. One way to do this is to compare the geometric-mean permeability of each radial grid cell to the frequency histogram of permeabilities for all cells. The permeability of the dominant petrophysical facies will closely match the permeability of one of the three original petrophysical facies. We use the capillary

pressure and relative permeability from the dominant petrophysical facies to populate each radial grid cell.

Perform flow simulations. Numerical simulations provide the key step to quantify the impact of carbonate rock heterogeneity on fluid flow (primary production, water flooding, or gas flooding). Such simulations are carried out on the constructed numerical pseudocores to estimate important parameters such as water cut, oil recovery factor, and recovery efficiency. Porosities, permeabilities, capillary pressures, and relative permeabilities for each radial grid cell are provided by the regriding process described in the previous step.

Our approach is to put a micro-injector at each radial cell location on the outside perimeter of the model and a micro-producer at each radial cell location on the inside perimeter of the model. Note that an inner part (4-in diameter) of the original numerical pseudocore has been drilled out to allow the arrangement of micro-producers (Figure 7 and 8). Flow can be modeled from the micro-injectors to the micro-producers. It is also possible to use analytical functions around the outside of the models to simulate the presence of an aquifer. Results of the flow simulations can be used to determine bulk, or system-scale values, such as residual oil saturation and relative permeability, which represent effective properties at the pseudocore scale.

Figure 11 illustrates the workflow of the pseudocore dynamics as well as scale differences between pseudocore models, conventional core plugs used in laboratory experiments, and microCTscan digital images. We emphasize that our pseudocore model is not built to resolve micron-scale features, which would require trillions of voxels; rather, it is generated at millimeter scale. The finer-scale features and their influences on flow in the pseudocores are carried out by assigning the corresponding properties (porosity, permeability, relative permeability, and capillary pressure, which may be obtained using pore-scale modeling) to each petrophysical facies at each voxel of the pseudocore model.

Wettability is controlled by inputting different capillary pressure and relative permeability curves. Figure 12 shows the oil saturation profile of a water-flooded numerical pseudocore under oil-wet and water-wet conditions. The visualization shows that the flow behavior and fluid distribution are fundamentally different: under oil-wet conditions, water flooding is a drainage process where water preferentially invades the conductive patches and vugs with smaller hydraulic resistances. Under water-wet conditions, water imbibes into the medium through the small pores in the matrix and tends to bypass the vugs.

J
J
J

Bulk, or system-scale, parameters such as residual oil saturation and relative permeability can be computed from the results of various time steps in the simulation by the reported flow rates. Figure 13 shows oil and water flow rates vs. time. Such output can be used to calculate effective relative permeability curves by

applying Darcy's law for radial flow. Oil saturations are known at each time step, and this is used to compute residual oil saturations and recovery factors. These values can be used directly in interwell- or field-scale simulations, assuming the volume of rock modeled is representative of a given reservoir rock type.

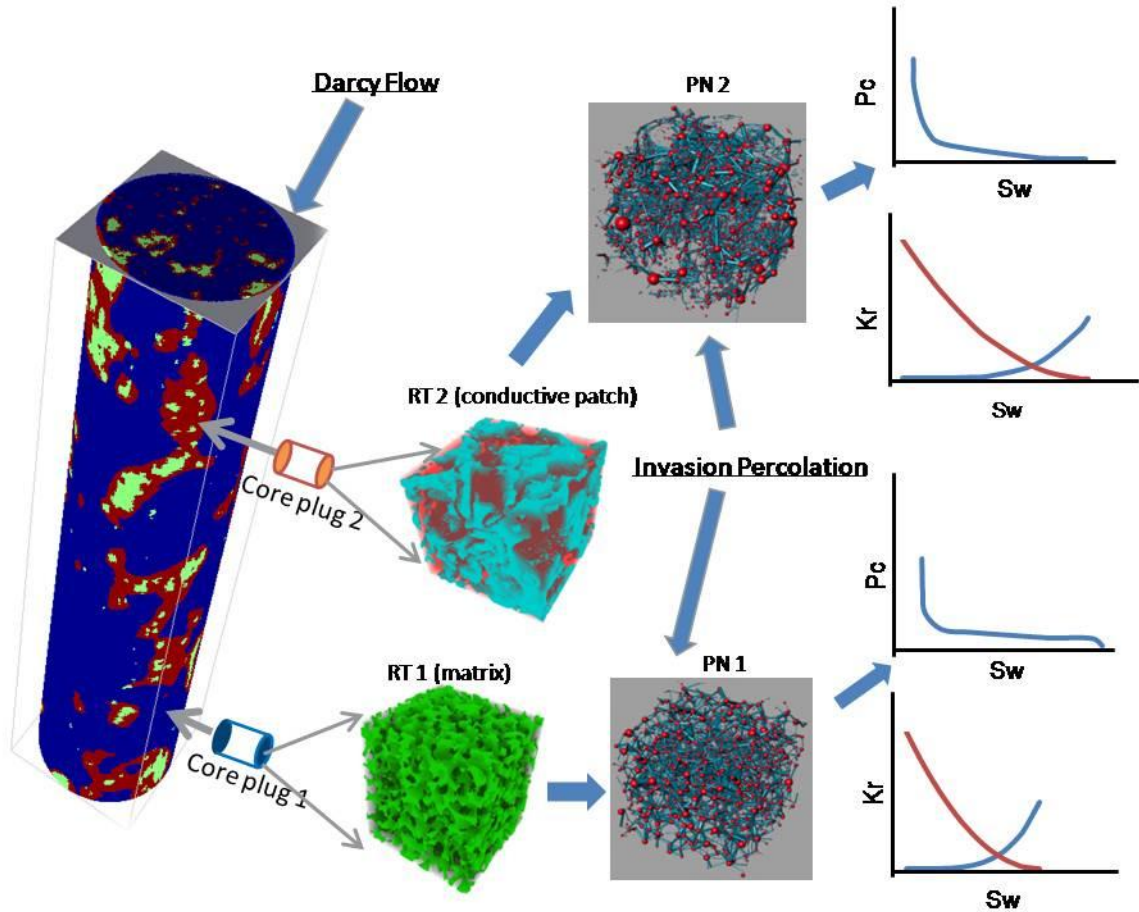


Fig. 11 Pseudocore workflow and scale differences. Core plugs 1 and 2 (left-hand side) are strategically located in petrophysical facies of dense rock matrix (blue) and conductive patches (red), respectively. Numerical pseudocore can be populated with dynamic properties (capillary pressure, P_c ; relative permeability, k_r) from SCAL work done on the core plugs (graphs on right-hand side). Another approach is to generate digital rock models from microCTscans (RT1 and RT2), pore network models (PN1 and PN2), and P_c and k_r plots using invasion-percolation flow modeling. Once the pseudocore has correctly distributed dynamic properties in 3D, Darcy flow modeling can be used to compute effective properties for the heterogeneous system.

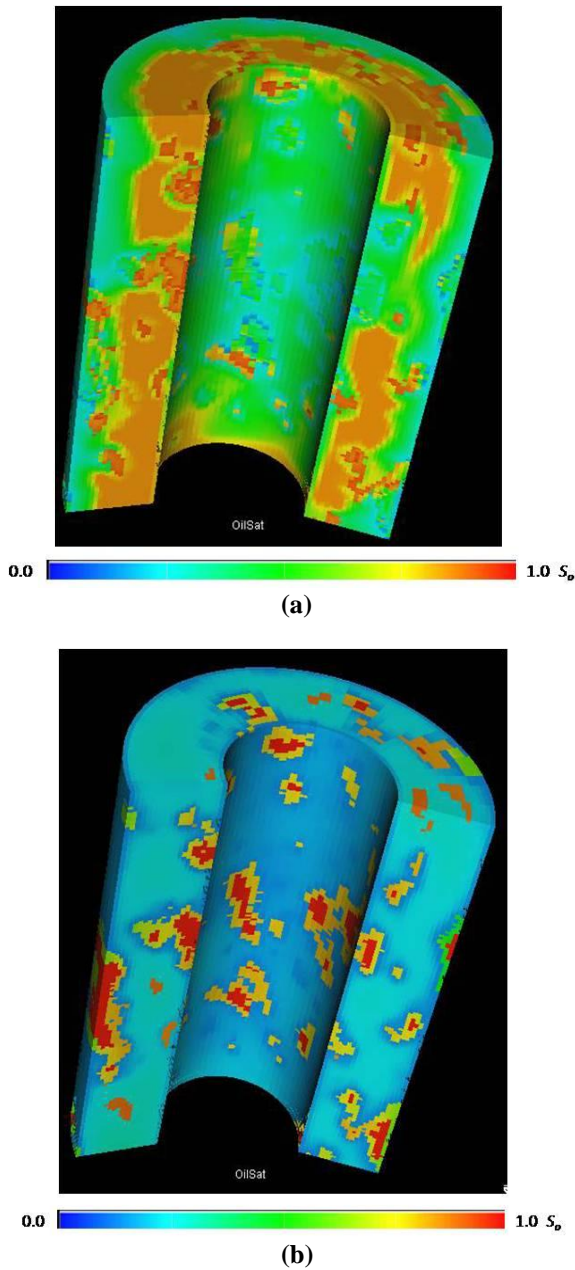


Fig. 12 Flow simulation results through numerical pseudocore for oil-wet (a) and water-wet (b) conditions. A line of micro-injectors of water surrounds the outer diameter, and a line of micro-producers surrounds the inner diameter of the pseudocore. Colors represent oil saturation (S_o). Heterogeneous breakthroughs are clearly shown in these flow models. The pseudocore is 1-ft (0.3-m) high, the outer diameter is 8.5 in (22 cm); the inner diameter is 4 in (10 cm).

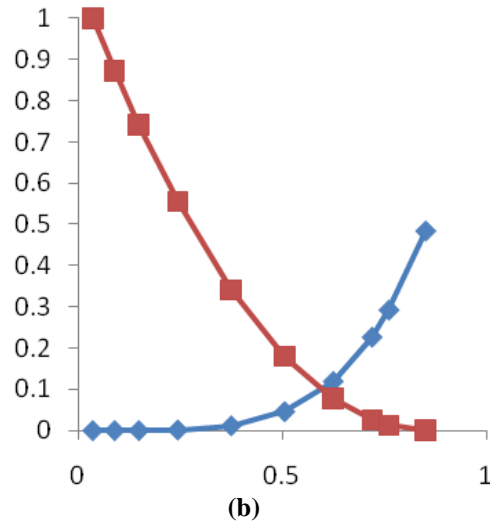
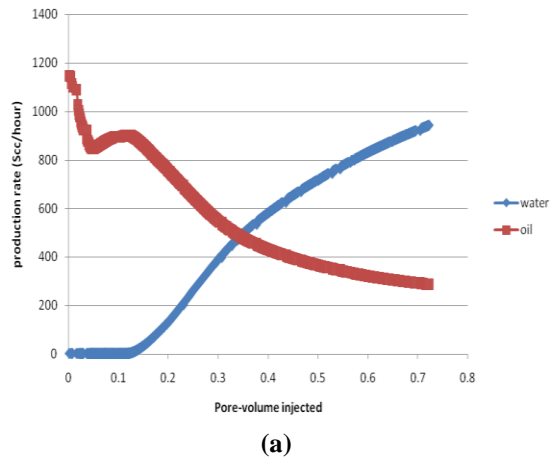


Fig. 13 (a) Water and oil production rates from the model shown in Figure 12(a). (b) Effective relative permeability curves (red = k_{ro} ; blue = k_{rw}) computed from modeled flow rates. The x axis is S_w .

J
J
J

CONCLUSIONS

Heterogeneity in carbonates and its impact on flow behavior have long been recognized. However, previous attempts to model such flow have commonly failed, mainly because other studies used core plugs or whole cores, and the sampled volumes are too small. This study captures flow heterogeneity in carbonates by focusing on textures recognized by borehole images, combined with digital rock samples generated by CTscan. We use these data to create 3D computer models of rocks and pores, known as numerical pseudocores, using new applications of multipoint statistics (MPS).

Numerical pseudocores are created using discrete-variable algorithms within MPS. Integer values are assigned to each petrophysical facies, for example, dense rock matrix is 0, vugs are 1, and conductive patches are 2. Digital rock samples are used as training images, that is, they are the quantitative templates used to guide the modeling of 3D textures in the pseudocore. Fullbore images, which are 360° views of the borehole wall generated by continuously variable MPS, surround numerical

pseudocores with cylindrical envelopes that condition the models. Each numerical pseudocore captures the heterogeneity of the digital rock samples and the fullbore images.

Numerical pseudocores address the question of small sample size for most digital rock models, especially those based on microCTscans. In fact, our technique adds value to such studies and provides a means to incorporate their results into larger-scale flow simulations.

Numerical pseudocores can be gridded into fluid-flow simulation models. For each petrophysical facies, capillary pressure and relative permeability curves are provided by conceptual models, special core analyses, or pore-network models. Bulk, or system-scale, properties such as effective residual oil saturations and relative permeabilities can be computed from flow-model results. These properties can be used to constrain interwell- or field-scale flow simulations.

REFERENCES

- Abu-Shiekah, I., Masalmeh, S.K., and Jing, X.D. 2007, Experimental investigation and modeling of waterflooding performance of a bioturbated carbonate formation. Society of Core Analysts. Paper SCA 2007-19.
- Behseresht, J., Bryant, S.L., and Sepehrnoori, K. 2007, Infinite-acting physically representative networks for capillarity-controlled displacements, SPE 110581: Society of Petroleum Engineers, presented at Annual Technical Conference and Exhibition, Anaheim, CA, 11-14 November.
- Bourke, L.T. 1993, Core permeability imaging: Its relevance to conventional core characterization and potential application to wireline measurement, *Marine and Petroleum Geology*, **10**: 318-324.
- Creusen, A., Maamari, K., Tull, S., Vahrenkamp, V., Mookerjee, A., and van Rijen, M. 2007, Property modeling small scale heterogeneity of carbonate facies, SPE 111451: Society of Petroleum Engineers, presented at Reservoir Characterization and Simulation Conference, Abu Dhabi, U.A.E., 28-31 October.
- Dehghani, K., Harris, P.M., Edwards, K.A., and Dees, W.T. 1999, Modeling a vuggy carbonate reservoir: *AAPG Bulletin* **83**: 19-42.
- Delhomme, J.P. 1992, A quantitative characterization of formation heterogeneities based on borehole image analysis. Trans. 33rd Symposium SPWLA. Paper T.
- Dvorkin, J., Kameda, A., Nur, A., Mese, A., and Tutuncu, A.N. 2003, Real time monitoring of permeability, elastic moduli and strength in sands and shales using digital rock physics, SPE 82246: Society of Petroleum Engineers, presented at European Formation Damage Conference, The Hague, Netherlands, 13-14 May.
- Gowelly, S. 2003, 3-D analysis of vug connectivity, Indian Basin field, New Mexico. MS thesis, Colorado School of Mines, Golden, CO.
- Guardiano, F., and Srivastava, R.M. 1993, Multivariate geostatistics: beyond bivariate moments. *Geostatistics-Troia*, A. Soares. Dordrecht, Netherlands, Kluwer Academic Publications **1**: 133-144.
- Hurley, N.F., and Zhang, T. 2009, Method to generate fullbore images using borehole images and multipoint statistics, SPE 120671: Society of Petroleum Engineers, presented at Middle East Oil & Gas Show and Conference, Bahrain, 15-18 March.
- Mathis, B., Leduc, J.P., and Vandenabeele, T. 2003, From the geologists' eyes to synthetic core descriptions: geological log modeling using well-log data (abs.) AAPG Annual Meeting, Salt Lake City, UT.
- Okabe, H., and Blunt, M.J. 2005, Pore space reconstruction using multiple-point statistics. *Journal of Petroleum Science and Engineering* **46**: 121-137.
- Oren, P.-E., and Bakke, S. 2002, Process based reconstruction of sandstones and prediction of

J
J
J

- transport properties. *Transport in Porous Media* **46**: 311-343.
- Rathod, A. 2003, Petrophysical analysis of the Thamama Group, Abu Dhabi, U.A.E. MS thesis, Colorado School of Mines, Golden, CO.
- Schindler, J. 2005, Quantification of vuggy porosity, Indian Basin field, New Mexico. MS thesis, Colorado School of Mines, Golden, CO.
- Strebelle, S. 2002, Conditional simulation of complex geological structures using multiple point statistics. *Mathematical Geology* **34**: 1-22.
- Tanprasat, S. 2005, Petrophysical analysis of vuggy porosity in the Shu'aiba Formation of the United Arab Emirates. MS thesis, Colorado School of Mines, Golden, CO.
- Tomutsa, L., and Radmilovic, V. 2007, Analysis of chalk petrophysical properties by means of submicron-scale pore imaging and modeling. *SPE Reservoir Evaluation and Engineering* **10**: 285-293.
- Vinegar, H.J. 1986, X-ray CT and NMR imaging of rocks. *Journal Of Petroleum Technology* 257-259.
- Wellington, S.L., and Vinegar, H.J. 1987, X-ray computerized tomography *Journal of Petroleum Technology* 885-898.
- Withjack, E.M., Devier, C., and Michael, G. 2003, The role of X-ray computed tomography in core analysis, SPE 83467: Society of Petroleum Engineers, presented at Western Region/AAPG Pacific Section Joint Meeting, Long Beach, CA, 19-24 May.
- Ye, S. -J., Rabiller, P., and Keskes, N. 1998, Automatic high resolution texture analysis on borehole imagery. *Transactions of the SPWLA Annual Logging Symposium*, M1-M14.
- Zhang, L., Nair, N., Jennings, J.W., and Bryant, S.L. 2005, Models and methods for determining transport properties of touching-vug carbonates, SPE 96027: Society of Petroleum Engineers, presented at Annual Technical Conference and Exhibition, Dallas, TX, 9-12 October.
- Zhang, T. 2006, Filter-based training image pattern classification for spatial pattern simulation. PhD dissertation, Stanford University, Palo Alto, CA.
- Zhang, T., Bombarde, S., Strebelle, S., and Oatney, E. 2006, 3D porosity modeling of a carbonate reservoir using continuous multiple-point statistics simulation. *SPE Journal* **11**: 375-379.

ABOUT THE AUTHORS

Tuanfeng Zhang is a Senior Research Scientist at Schlumberger-Doll Research, Cambridge, MA, USA. His research interests include geomodeling, reservoir modeling and characterization, geostatistics, spatial statistics and its applications. He was an associate professor in Xian Petroleum Institute, China, from 1995 to 2000. Later, he studied at Stanford University from 2002 to 2006. He earned his MS degree in petroleum engineering in 2002 and his PhD in geological and environmental sciences in 2006.

Neil Hurley is a Scientific Advisor at Schlumberger-Doll Research, Cambridge, MA, USA. His research interests include borehole images and carbonate reservoir characterization. He worked for Conoco Inc. and Marathon Oil Company from 1978-1996, and he is Emeritus Professor, retired from the Colorado School of Mines, 2006. He earned his BS degrees in geology and petroleum engineering from the University of Southern California in 1976, his MS degree in geology from the University of Wisconsin in 1978, and his PhD in geology from the University of Michigan in 1986.

Weishu Zhao is a Post-Doctoral Scientist at Schlumberger-Doll Research, Cambridge, MA, USA. His research interests include transport phenomena in porous media, pore-scale modeling of multiphase flow and reservoir simulation. He earned his MS degree (2002) and PhD (2006) in chemical engineering at the University of Waterloo, Ontario, Canada.

J
J
J